Energy transfer processes in Er^{3+}-doped and Er^{3+},Pr^{3+}-codoped ZBLAN glasses

P. S. Golding, S. D. Jackson, T. A. King, and M. Pollnau*
Laser Photonics Group, Schuster Laboratory, Department of Physics and Astronomy, University of Manchester, Manchester M13 9PL, United Kingdom

(Received 26 October 1999; revised manuscript received 10 February 2000)

We present a detailed characterization of energy transfer processes in Er^{3+}-doped and Er^{3+},Pr^{3+}-codoped ZBLAN bulk glasses. For several Er^{3+} (0.25–8.75 mol%) and Pr^{3+} (0.25–1.55 mol%) concentrations, we investigate energy transfer upconversion (ETU) and cross relaxation in Er^{3+} as well as energy transfer (ET) from Er^{3+} to the Pr^{3+} codopant. The measured parameters of ETU from the Er^{3+} $^4I_{13/2}$ and $^4I_{11/2}$ levels are comparable to those of $LiYF_4$:Er^{3+}. ETU from $^4I_{13/2}$, in particular, possesses a factor of 3 larger probability than ETU from $^4I_{11/2}$. The parameters of ET from the Er^{3+} $^4I_{13/2}$ and $^4I_{11/2}$ levels to the Pr^{3+} codopant are larger than the corresponding ETU parameters. ET effectively quenches the $^4I_{13/2}$ intrinsic lifetime of 9 ms down to 20 μs for the highest Er^{3+} and Pr^{3+} concentrations investigated, and is more efficient than ET from $^4I_{11/2}$, because the corresponding absorption transition in Pr^{3+} has a large oscillator strength and back transfer is inhibited by fast multiphonon relaxation from the corresponding Pr^{3+} level. In both cases, the ET parameters depend on Er^{3+} concentration in a similar way as the ETU parameters but depend only weakly on Pr^{3+} concentration. This shows that energy migration within the Er^{3+} $^4I_{13/2}$ and $^4I_{11/2}$ levels is fast. The presented results are important for the choice of the appropriate operational regime of the erbium 3-μm fiber laser.

I. INTRODUCTION

After the first successful descriptions of energy transfer processes by Förster[1] and Dexter,[2] strong interest in the spectroscopic investigation of these processes has proceeded. One possible manifestation of an energy transfer process is the occurrence of visible luminescence from a sample after infrared excitation and the subsequent energy transfer upconversion (ETU) to the emitting state.[3–5] The influences of energy transfer processes affect the performance of many rare-earth-doped solid-state lasers. For instance, these processes can be a source of loss if originating in the upper laser level.[6,7] However, these processes can be beneficial, e.g., for sensitizing the lasing ion by energy transfer (ET) from a codopant,[8,9] for quenching the lower laser level by ET to a codopant,[10,11] or for ETU of the pump excitation to a high-lying upper laser level.[12,13] A quantitative understanding of the relevant energy transfer processes is, therefore, required for optimizing the corresponding laser system.

The erbium 3-μm laser which is of interest for medical applications[14–16] is based on a simple four-level laser scheme, see Fig. 1. Since the $^4I_{13/2}$ lower laser level is metastable, however, significant excitation is accumulated in this level and, due to the CW threshold condition, also in the $^4I_{11/2}$ upper laser level. Owing to the equal energetic spacing of several multiplet-to-multiplet transitions, energy transfer processes occur from these levels. An important process is ETU from $^4I_{13/2}$, which recycles energy from the lower to the upper laser level. Based on this process, the 3-μm crystal laser is operated CW even for unfavorable lifetime ratios of the laser levels[17] and output powers exceeding 1 W have been obtained.[18,19] Energy recycling by way of ETU from the $^4I_{13/2}$ level enhances the limit of the slope efficiency to twice the Stokes efficiency.[20,21] On the other hand, lifetime quenching of the lower laser level by ET to a codopant ion such as Pr^{3+} (see Fig. 1) limits the slope efficiency[10] to values below the Stokes limit.

ZBLAN glass fiber also serves as a useful host for Er^{3+} ions for an efficient 3-μm laser, providing, as a result of its geometry, a high-brightness laser beam and greatly reduced thermal effects. The operation of the Er^{3+}-doped ZBLAN fiber laser is often limited, however, by ground-state bleaching with the consequence of undesired excited-state absorption (ESA) from the $^4I_{13/2}$ and $^4I_{11/2}$ laser levels.[22–24] Under intense pumping, ESA can be exploited in cascade-lasing regimes,[25,26] but under pump excitation with low-brightness

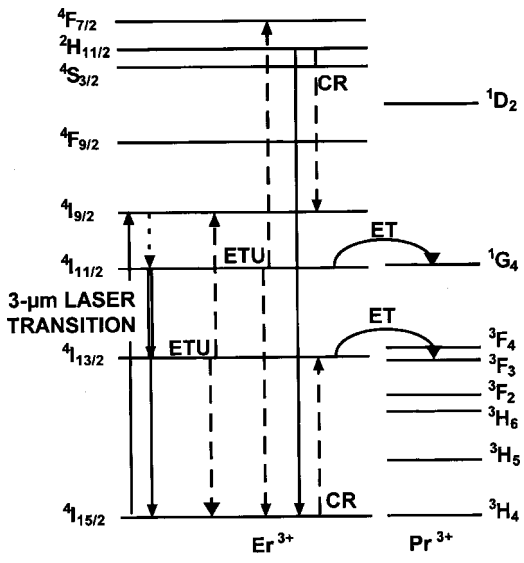

FIG. 1. Partial energy level diagram of Er^{3+} and Pr^{3+} in ZBLAN glass indicating the simple four-level scheme of the erbium 3-μm laser (left-hand side), ETU and CR processes from the Er^{3+} $^4I_{13/2}$, $^4I_{11/2}$, and $^4S_{3/2}/^2H_{11/2}$ levels, as well as ET processes from Er^{3+} to Pr^{3+}.

diode lasers the limitation can only be overcome by either of two different operational regimes: quenching of the $^4I_{13/2}$ lifetime by ET to a Pr^{3+} codopant or energy recycling from $^4I_{13/2}$ by ETU (Fig. 1). The former regime has recently been shown to be applicable[27] and output powers at 3 μm approaching 1 W (Ref. 28) or even 2 W (Ref. 29) have been achieved in double-clad geometries.[30] Lasers based on singly erbium-doped ZBLAN fibers and bulk glasses have also been demonstrated.[31,32] It has been an open question in which of these two regimes the fiber laser can be operated more efficiently.

In order to prepare the spectroscopic ground for an answer to this question, we have measured the intrinsic lifetimes of the Er^{3+} $^4I_{13/2}$, $^4I_{11/2}$ and $^4S_{3/2}/^2H_{11/2}$ levels and investigated the major energy transfer processes such as ETU from the Er^{3+} $^4I_{13/2}$ and $^4I_{11/2}$ laser levels, ET from these levels to the corresponding levels of a Pr^{3+} codopant, and cross relaxation (CR) from the thermally-coupled Er^{3+} $^4S_{3/2}/^2H_{11/2}$ levels. The macroscopic energy transfer parameters of all these processes are derived and their dependence on Er^{3+} and Pr^{3+} concentrations is investigated. Consequences for the choice of the appropriate operational regime of the erbium 3-μm fiber laser are established.

II. EXPERIMENT

Lifetimes as well as the parameters of ETU, CR, and ET for Er^{3+}-doped and Er^{3+},Pr^{3+}-codoped in ZBLAN bulk glasses (Le Verre Fluoré, France) were determined by measuring luminescence decay from the $^4I_{13/2}$, $^4I_{11/2}$ levels and the thermally coupled $^4S_{3/2}/^2H_{11/2}$ levels to the $^4I_{15/2}$ ground state following direct excitation of these levels at 532, 979, and 1510 nm, respectively. The samples studied in this investigation comprised of four Er^{3+}-doped samples of concentrations 0.25, 1.25, 5, and 8.75 mol%, and six Er^{3+}, Pr^{3+}-codoped samples: Er^{3+} 8.75 mol%, Pr^{3+} 0.25, 0.5, and 1.25 mol%, and Er^{3+} 5 mol%, Pr^{3+} 0.25, 0.5, and 1.55 mol% (1 mol%$=1.6\times10^{20}\,cm^{-3}$). Each sample had dimensions of $10\times10\times5\ mm^3$ and was polished on all faces.

The excitation source for the spectroscopic measurements was an in-house KTP optical parametric oscillator (OPO) pumped by a frequency-doubled, 10 Hz, Q-switched laser (Spectron SL802G) at 532 nm. The OPO consisted of a two-crystal, walk-off-compensated cavity[33] (see Fig. 2). A signal tuning range of 770 to 980 nm with the associated idler wavelength of 1700 to 1160 nm was attainable. Two mirror sets were used; one that was highly transmitting at the idler wavelength of 1500 nm and highly reflecting at the signal wavelength of 824 nm, and a second with a high transmission at 980 nm and a high reflection at 1160 nm. This source provided pump light which was tunable across the absorption regions of the $^4I_{13/2}$ and $^4I_{11/2}$ levels, with maximum output energies of 1 mJ and a pulse length of approximately 6 ns that allowed each level to be excited in a time scale significantly shorter than its lifetime. Furthermore, since each level could be directly excited, it was possible to determine lifetimes systematically allowing a simple and accurate method for determining the temporally-resolved spectroscopic characteristics of each sample. Since the bandwidth of the OPO was approximately 5 nm, the majority of the inhomogeneous bandwidth was excited and hence the emission from most Er^{3+} sites was measured.

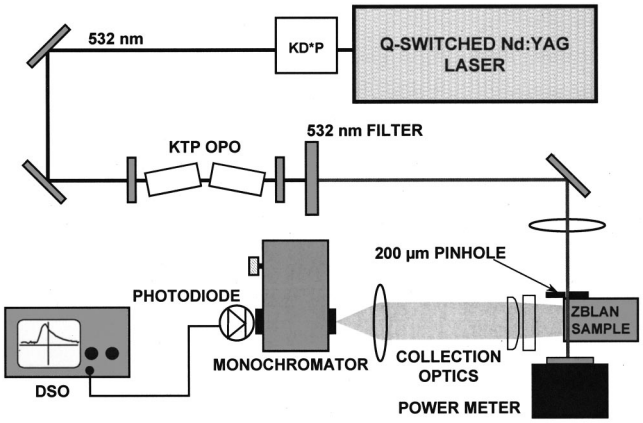

FIG. 2. Experimental setup for the measurement of the temporally- and spectroscopically-resolved luminescence from the ZBLAN:Er^{3+} and ZBLAN:Er^{3+}:Pr^{3+} glass samples.

To excite the $^4I_{13/2}$ level, a center wavelength of the pump of 1510 nm was selected. For the $^4I_{11/2}$ level a center wavelength of the pump of 979 nm was used, because ground-state absorption (GSA) was sufficiently high, but ESA was significantly less than GSA due to the relatively small excitation density and the small ESA cross-section at this wavelength.[23] The lifetime of the thermally coupled $^4S_{3/2}/^2H_{11/2}$ levels was measured after direct excitation by the second harmonic of the *Q*-switched Nd:YAG laser at 532 nm.

The pump beam was focused by an 8-cm lens and sent through a 200-μm pinhole to give a known excitation volume with a relatively homogeneously excited cross section and directed through the sample close to one of its surfaces, see Fig. 2. Luminescence was then detected from the surface closest to the excitation path to ensure that reabsorption effects did not affect the decay-time data. The luminescence from the samples was imaged onto the entrance slit of a 30 cm monochromater, and the resulting signal was detected using a InGaAs photodiode (Hamamatsu G5746-01) to detect the $^4I_{13/2}$ luminescence at 1560 nm and a silicon photodiode (IPL 10530 DAL) to detect the 1010 nm ($^4I_{11/2}$) and 550 nm ($^4S_{3/2}$) luminescences. The overall bandwidth of the detected luminescence was measured to be approximately 4 nm. Signals were averaged over 512 shots with use of a Hewlett-Packard 54522A digital storage oscilloscope. Decay curves were measured for different pump energies incident on the crystal surface, and the transmitted pump energies were recorded.

III. RESULTS

A. Cross relaxation in Er^{3+}-doped ZBLAN

We first investigate the luminescent decay from the $^4S_{3/2}/^2H_{11/2}$ levels, because the result is important for the determination of the parameter of the ETU process from the $^4I_{11/2}$ level (see later). The $^4S_{3/2}$ level is in thermal equilibrium with the $^2H_{11/2}$ level, therefore, after excitation, the population relaxes to the Boltzmann distribution within the two levels. At high Er^{3+} concentrations, the luminescent life-

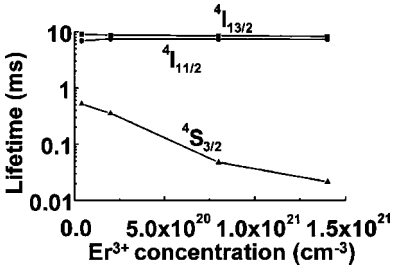

FIG. 3. Intrinsic lifetimes of the $^4I_{13/2}$ (squares) and $^4I_{11/2}$ (circles) levels as well as the effective lifetime of the $^4S_{3/2}/^2H_{11/2}$ levels (triangles) in ZBLAN:Er^{3+} for different Er^{3+} concentrations.

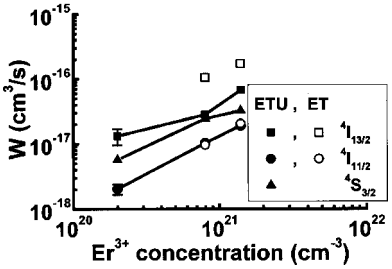

FIG. 4. Macroscopic parameters (solid symbols) of ETU from Er^{3+} $^4I_{13/2}$ and $^4I_{11/2}$ as well as CR from Er^{3+} $^4S_{3/2}/^2H_{11/2}$ vs. Er^{3+} concentration. Also shown are the macroscopic parameters (open symbols) of ET from Er^{3+} $^4I_{13/2}$ and $^4I_{11/2}$ to the Pr^{3+} codopant for a Pr^{3+} concentration of $8\times10^{19}\,\mathrm{cm}^{-3}$.

time of these levels is shortened as a result of the CR processes $(^2H_{11/2}, ^4I_{15/2}) \rightarrow (^4I_{9/2}, ^4I_{13/2})$ and $(^2H_{11/2}, ^4I_{15/2}) \rightarrow (^4{}_{13/2}, ^4I_{9/2})$. The effect of the Er^{3+} concentration upon the luminescent lifetime of the $^4S_{3/2}/^2H_{11/2}$ levels is shown in Fig. 3. The observed luminescence from the $^4S_{3/2}/^2H_{11/2}$ levels shows a dramatic reduction in lifetime with a value of $518\pm6\,\mu$s for an Er^{3+} concentration of 0.25 mol%($4\times10^{19}\,\mathrm{cm}^{-3}$) falling to $21\pm1\,\mu$s for an Er^{3+} concentration of 8.75 mol%($1.4\times10^{21}\,\mathrm{cm}^{-3}$). Extrapolation of the curve toward zero Er^{3+} concentration provides an intrinsic lifetime of 586 μs, in good agreement with Ref. 34 which states a lifetime of 570 μs.

The rate of the CR process, R_{CR}, can be described by

$$R_{\mathrm{CR}} = W_{\mathrm{CR}} N(^4S_{3/2}) N(^4I_{15/2}), \tag{1}$$

where W_{CR} is the macroscopic CR parameter, $N(^4S_{3/2})$ is the population density of the $^4S_{3/2}/^2H_{11/2}$ levels, and $N(^4I_{15/2})$ is the population density of the $^4I_{15/2}$ ground state. In our experiment, the ground-state bleaching and excitation of the $^4S_{3/2}/^2H_{11/2}$ levels is small. It follows that the ground-state population density can be approximated by the Er^{3+} concentration $N(\mathrm{Er})$ in the sample, the rate R_{CR} increases linearly with pump power and excitation in the $^4S_{3/2}/^2H_{11/2}$ levels, and the resulting effective luminescent lifetime $\tau_{\mathrm{eff}}(^4S_{3/2})$ can be described as follows:

$$1/\tau_{\mathrm{eff}}(^4S_{3/2}) = 1/\tau(^4S_{3/2}) + W_{\mathrm{CR}} N(\mathrm{Er}), \tag{2}$$

where $\tau(^4S_{3/2})$ is the intrinsic lifetime of the $^4S_{3/2}/^2H_{11/2}$ levels. The CR parameters determined from the measured lifetime quenching are given in Table I and Fig. 4.

B. Energy transfer upconversion in Er^{3+}-doped ZBLAN

The luminescent decay measured from the $^4I_{11/2}$ and $^4I_{13/2}$ levels of Er^{3+} can be considered as being composed of two separate parts. As can be seen in Fig. 5(a), a fast nonexponential section is observed at the beginning of the decay that contains a strong contribution from fast ion–ion interactions. For a given sample, the magnitude of the ETU-induced part of the decay increases with increasing initial excitation density N_0 of the corresponding excited level. This fast decay is followed by a slower exponential decay that results solely from the intrinsic decay rate of the level (i.e., the decay rate of an isolated ion) and is independent of the initial pump excitation. To determine the lifetime of the excited levels a linear fit is applied to the last portion of the $\ln(I/I_0)$ graph, with care taken not to include the part of the decay that involves ion–ion interaction.

Figure 3 shows the measured luminescent lifetimes of the $^4I_{13/2}$ and $^4I_{11/2}$ levels. The $^4I_{11/2}$ level has a shorter lifetime than the $^4I_{13/2}$ level, commensurate with a previous investigation.[34] For the lowest doped samples, lifetimes of 6.9 ± 0.1 ms and 9.0 ± 0.2 ms, respectively, were measured. On increasing the Er^{3+} concentration, the $^4I_{11/2}$ lifetime is seen to increase and the $^4I_{13/2}$ lifetime to decrease. Other authors studying Er^{3+}-doped fluorozirconate glass have observed small fluctuations in these lifetimes over a concentration range of 0.8 to 18 mol%.[35] This variation may be caused by a slight change in the maximum phonon energies with glass composition, which will affect the multiphonon decay rates, or an energy transfer process to the host material.[36]

TABLE I. Values of the measured ETU, CR, and ET parameters ($10^{-17}\,\mathrm{cm}^3\,\mathrm{s}^{-1}$) for the different investigated Er^{3+} and Pr^{3+} concentrations ($10^{20}\,\mathrm{cm}^{-3}$).

Er^{3+} conc.	Pr^{3+} conc.	ETU $^4I_{13/2}$	ETU $^4I_{11/2}$	CR $^4S_{3/2}$	ET $^4I_{13/2}$	ET $^4I_{11/2}$
0.4	0			0.6		
2	0	1.3	0.2	0.6		
8	0	2.8	1.0	2.4		
	0.4				9.0	0.9
	0.8				10.6	1.0
	2.5				13.2	1.0
14	0	6.7	1.9	3.3		
	0.4				16.8	2.1
	0.8				17.2	2.0
	2.0				20.5	2.2

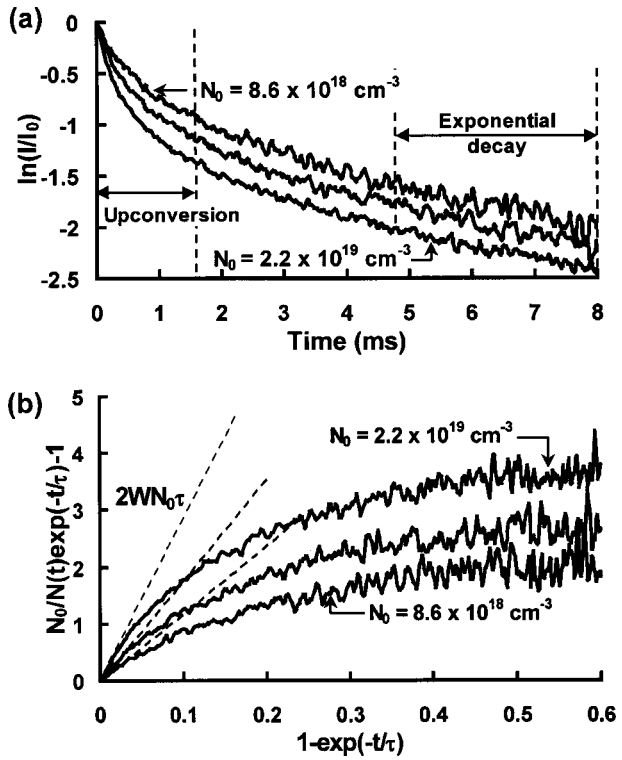

FIG. 5. (a) Example of the measured (and normalized) luminescence-decay characteristic from the Er^{3+} $^4I_{13/2}$ level at a wavelength of 1560 nm in ZBLAN:8.75 mol% Er^{3+} for different excitation densities. Indicated are the portions of the measured luminescence characteristic that were used for the determination of the ETU parameters and the intrinsic lifetimes. (b) Linearization of the decay curves of (a) with respect to the ETU parameters *W*. Indicated are the slopes that lead to the determination of the ETU parameters. This method is taken from Ref. 37. N_0 is the initial excitation density at $t=0$ ms.

ETU parameters were calculated according to a previously published method,[37] as follows. If N represents the time-dependent population density of the excited $^4I_{13/2}$ level, then the rate equation for N is given by

$$\frac{dN}{dt} = -\frac{N}{\tau} - 2W_{\mathrm{ETU}}N^2, \tag{3}$$

where τ is its intrinsic lifetime, and W_{ETU} is the macroscopic ETU parameter relating to the process $(^4I_{13/2}, ^4I_{13/2}) \rightarrow (^4I_{15/2}, ^4I_{9/2})$. With $N(t=0)=N_0$, integration yields[38]

$$N(t) = \frac{N_0 \exp(-t/\tau)}{1 + 2W_{\mathrm{ETU}}N_0\tau[1-\exp(-t/\tau)]}, \tag{4}$$

or

$$[N_0/N(t)]\exp(-t/\tau) - 1 = 2W_{\mathrm{ETU}}N_0\tau[1-\exp(-t/\tau)]. \tag{5}$$

A plot of $[N_0/N(t)]\exp(-t/\tau)-1$ vs. $[1-\exp(-t/\tau)]$ will, therefore, give a gradient of $2W_{\mathrm{ETU}}N_0\tau$. This is only correct as long as the decay can be described by Eq. (3), i.e., in the first temporal part of the decay when only the directly-pumped level is significantly excited and processes involving other excited levels, especially those processes which repopulate the level under investigation, are negligible. After a certain time, the curves plotted in this way will deviate from the linear behavior according to Eq. (5) because of the increasing influence of those processes. By using only the data in the first temporal part of the decay we can avoid this complication.[37] If we considered the complete decay curve, a more complex rate–equation system of ZBLAN:Er^{3+} with a corresponding number of parameters, parameter values, and error margins would have to be taken into account. Most notably, the evaluation of a transfer parameter would depend on the other transfer parameters, which are themselves subject to the investigation. Such a method would be less precise than the one chosen here.

A plot of the data of Fig. 5(a) in a $[N_0/N(t)]\exp(-t/\tau) - 1$ vs. $[1-\exp(-t/\tau)]$ representation for different pump energies, in this case for the decay from the $^4I_{13/2}$ level in ZBLAN:8.75 mol% Er^{3+}, is shown in Fig. 5(b), where $N_0/N(t)$ is the luminescence signal at the beginning of the decay ratioed to the signal at time t, and τ is taken to be the lifetime of the lowest doped sample. A straight-line fit to the initial linear part of the resulting graph gives a gradient equal to $2W_{\mathrm{ETU}}N_0\tau$. N_0 is calculated by knowing the absorbed photon density, i.e., the energy absorbed within a pulse, the excited volume determined by the pinhole and the thickness of the sample, and the pump–photon energy.

ETU from the $^4I_{13/2}$ level populates the $^4I_{9/2}$ level from where most of the excitation decays by fast multiphonon relaxation to the metastable $^4I_{11/2}$ level. Repopulation of the $^4I_{13/2}$ level from $^4I_{11/2}$ occurs at a time scale which is large compared to the time scale used for extracting the ETU parameters; see Fig. 5(a). Direct back transfer from the $^4I_{9/2}$ level by the CR process $(^4I_{9/2}, ^4I_{15/2}) \rightarrow (^4I_{13/2}, ^4I_{13/2})$ has a relatively small influence because of the relatively short lifetime of the $^4I_{9/2}$ level (calculated from Ref. 36 to be < 20 μs) as a result of relatively fast nonradiative relaxation from this level to the $^4I_{11/2}$ level. Investigations in $LiYF_4$:Er^{3+} have established[37] that the direct back transfer changes the parameter of ETU from $^4I_{13/2}$ by less than 10% for the dopant concentrations of interest in the present article. This deviation is in the order of the error margin of the ETU parameter and is, therefore, neglected in our evaluation. The parameters of ETU from $^4I_{13/2}$ are, therefore, derived from Fig. 5(b) by assuming a slope of $2W_{\mathrm{ETU}}N_0\tau$, as suggested by Eq. (5).

The situation is different for the luminescent decay curve and ETU process, $(^4I_{11/2}, ^4I_{11/2}) \rightarrow (^4I_{15/2}, ^4F_{7/2})$, from the $^4I_{11/2}$ level. ETU from this level populates the $^4F_{7/2}$ level from where the excitation relaxes by fast multiphonon decay to the $^4S_{3/2}/^2H_{11/2}$ levels. At a low dopant concentration, these levels decay mostly radiatively to the $^4I_{15/2}$ and $^4I_{13/2}$ levels, i.e., there is no significant back transfer to $^4I_{11/2}$ within the time scale relevant for the determination of the parameter of ETU from $^4I_{11/2}$. At a higher dopant concentration, however, CR from the $^4S_{3/2}/^2H_{11/2}$ levels discussed above, leads to a fast back transfer into the $^4I_{9/2}$ level and further into the $^4I_{11/2}$ level by multiphonon relaxation. If the effective lifetime of the $^4S_{3/2}/^2H_{11/2}$ levels is short, most of the upconverted excitation is transferred back to $^4I_{11/2}$ within the relevant time scale. The result is that only one excitation is removed from the $^4I_{11/2}$ level by each ETU process and the factor of 2 in Eq. (3) reduces to a factor of 1. For intermediate dopant concentrations, CR and luminescent decay

compete for the depletion of the $^4S_{3/2}/^2H_{11/2}$ levels. We can define a branching ratio, β, for the part that decays by CR,

$$\beta = \frac{W_{CR}N(^4S_{3/2})N(\mathrm{Er})}{N(^4S_{3/2})/\tau(^4S_{3/2}) + W_{CR}N(^4S_{3/2})N(\mathrm{Er})} = 1 - \frac{\tau_{eff}(^4S_{3/2})}{\tau(^4S_{3/2})}. \quad (6)$$

It follows that Eq. (3) changes to

$$\frac{dN(^4I_{11/2})}{dt} = -\frac{N(^4I_{11/2})}{\tau(^4I_{11/2})} - (2-\beta)W_{ETU}N^2(^4I_{11/2}). \quad (7)$$

The initial slope which is derived from Eq. (5) and indicated in Fig. 5(b) then reduces to $[1+\tau_{eff}(^4S_{3/2})/\tau(^4S_{3/2})]W_{ETU}N_0\tau$. The parameters of ETU from the $^4I_{11/2}$ level are evaluated from the data of Fig. 5(b) by assuming this slope and using the effective lifetimes of the $^4S_{3/2}/^2H_{11/2}$ levels of Fig. 3 and the intrinsic lifetime of 586 μs.

Equation (7) holds true for $1/\tau_{eff}(^4S_{3/2}) \gg 1/\tau(^4I_{11/2}) + W_{ETU}N^2(^4I_{11/2})$, i.e., for situations where the back transfer is immediate with respect to the depletion of the $^4I_{11/2}$ level. This is the case for the highly Er^{3+}-doped samples investigated. For the lowest dopant concentration for which ETU is investigated, this approximation is not valid, but since for this concentration $\tau_{eff}(^4S_{3/2})$ approaches $\tau(^4S_{3/2})$, it follows that β vanishes and Eq. (7) reduces to Eq. (3).

Without considering back transfer the derived ETU parameter would be correct only for a low dopant concentration, but would be a factor of 2 too small for a high dopant concentration. Using the parameters of ZBLAN:Er^{3+} and a predefined ETU parameter, we have solved an extended rate–equation system (see, e.g., Ref. 27) numerically and generated luminescent decay curves with and without considering the influence of back transfer by CR. This method confirmed that the consideration of back transfer as in Eqs. (6) and (7) leads to a much higher precision in the evaluation of the parameter of ETU from $^4I_{11/2}$.

The ETU parameters for the $^4I_{11/2}$ and $^4I_{13/2}$ levels calculated in the different ways described above are given in Table I and Fig. 4 for several Er^{3+} concentrations. It can be seen that the probability of ETU from the $^4I_{13/2}$ level is higher by approximately a factor of 3 times that of the $^4I_{11/2}$ level. The ETU parameters increase with increasing Er^{3+} concentration.

C. Energy transfer in Er^{3+},Pr^{3+}-codoped ZBLAN

The luminescent decay curves after excitation with the OPO source for the Er^{3+},Pr^{3+}-codoped samples were obtained in a similar manner to the Er^{3+}-doped samples. Figure 6(a) shows the influence of the Pr^{3+} codopant on the Er^{3+} $^4I_{13/2}$ and $^4I_{11/2}$ lifetimes. A significant reduction in the lifetime of the $^4I_{13/2}$ level is observed following the addition of a small amount of Pr^{3+}, while the lifetime of $^4I_{11/2}$ level is affected to a lesser degree.

Using the same analysis as for the $^4S_{3/2}/^2H_{11/2}$ luminescent decay described above, a rate for the ET process, R_{ET}, can be described by

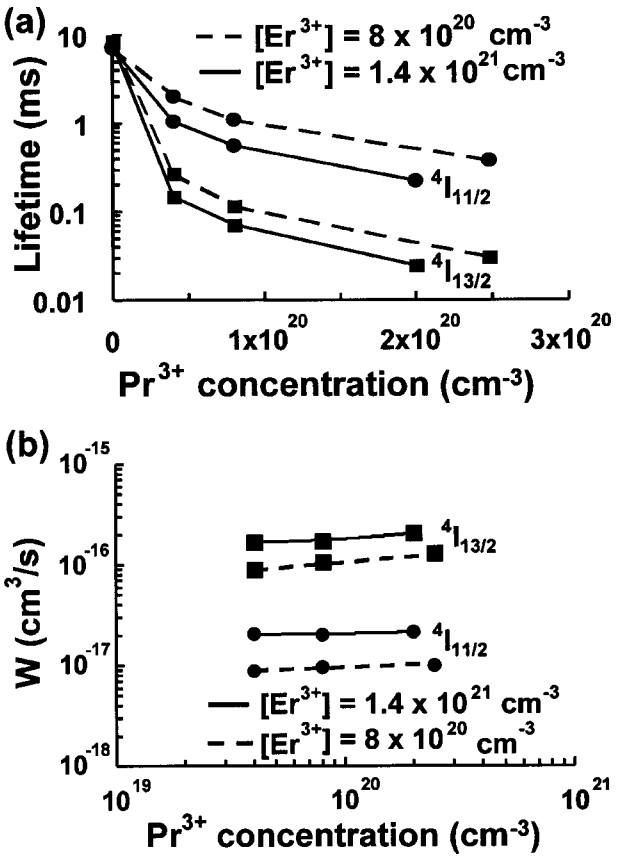

FIG. 6. (a) Measured lifetimes and (b) macroscopic parameters of ET from the Er^{3+} $^4I_{13/2}$ and $^4I_{11/2}$ levels to the Pr^{3+} codopant, as a function of Pr^{3+} concentration and for two different Er^{3+} concentrations.

$$R_{ET} = W_{ET}N(\mathrm{Er}^*)N(^3H_4), \quad (8)$$

where W_{ET} is the macroscopic ET parameter, $N(\mathrm{Er}^*)$, is the excited-state population density of a given Er^{3+} level, and $N(^3H_4)$ is the population density of the $^3H_4$ ground state of Pr^{3+}. Assuming negligible excitation of the Pr^{3+} ions, the resulting luminescent decay from the Er^{3+} levels can be described as follows:

$$1/\tau_{eff}(\mathrm{Er}^*) = 1/\tau(\mathrm{Er}^*) + W_{ET}N(\mathrm{Pr}), \quad (9)$$

where $\tau_{eff}(\mathrm{Er}^*)$ is the effective lifetime of the excited level of Er^{3+} in which ET is observed, $\tau(\mathrm{Er}^*)$ is the intrinsic lifetime of the same level, and $N(\mathrm{Pr})$ is the Pr^{3+} concentration in the sample. Using Eq. (9), the ET parameters W_{ET} have been calculated for the samples under investigation, see Table I and Fig. 6(b). The degree of ET to Pr^{3+} is found to be much higher for the $^4I_{13/2}$ than for the $^4I_{11/2}$ level of Er^{3+}.

IV. DISCUSSION

A. Relative strengths of transfer parameters

We first compare the strengths of the investigated ETU, CR, and ET parameters relative to each other in a simplified model. For the most common energy transfer mechanism of electric-dipole–electric-dipole interaction, the values for the transfer parameters are proportional to the product of the oscillator strengths of the corresponding emission and ab-

TABLE II. Oscillator strengths [10^8] for electric–dipole transitions of Er^{3+} and Pr^{3+} from Ref. 39. The value of the $^4I_{11/2} \leftrightarrow {}^4F_{7/2}$ transition which is denoted by an asterisk is not given in Ref. 39. From a comparison with $LiYF_4$ (Ref. 40), it is assumed here to have the same values as the $^4I_{15/2} \leftrightarrow {}^4I_{11/2}$ transition.

Ion	Transition	YLF	Oscillator Strength
Er^{3+}	$^4I_{15/2} \leftrightarrow {}^4I_{13/2}$	135.8	100
	$^4I_{15/2} \leftrightarrow {}^4I_{11/2}$	126.7	44
	$^4I_{15/2} \leftrightarrow {}^4I_{9/2}$	54.3	33
	$^4I_{13/2} \leftrightarrow {}^4I_{9/2}$	48.5	45
	$^4I_{13/2} \leftrightarrow {}^4S_{3/2}$	474.2	42
	$^4I_{13/2} \leftrightarrow {}^2H_{11/2}$	58.2	30
	$^4I_{11/2} \leftrightarrow {}^4F_{7/2}$	129.6	44*
	$^4I_{9/2} \leftrightarrow {}^4S_{3/2}$	52.1	34
	$^4I_{9/2} \leftrightarrow {}^2H_{11/2}$	43.8	95
Pr^{3+}	$^3H_4 \leftrightarrow {}^3F_3$		840
	$^3H_4 \leftrightarrow {}^1G_4$		21

sorption transitions.[2,4] Table II lists the oscillator strengths for the Er^{3+} and Pr^{3+} transitions[39] that are relevant for the transfer processes investigated experimentally in Secs. II and III.

For the ETU process $(^4I_{13/2}, {}^4I_{13/2}) \rightarrow (^4I_{15/2}, {}^4I_{9/2})$, the product of the oscillator strengths $(^4I_{15/2} \leftrightarrow {}^4I_{13/2}) \times (^4I_{13/2} \leftrightarrow {}^4I_{9/2})$ of Table II is 4500×10^{16}, which is higher than the product of 1963×10^{16} for the ETU process $(^4I_{11/2}, {}^4I_{11/2}) \rightarrow (^4I_{15/2}, {}^4F_{7/2})$, in qualitative agreement with the experimental results for the ETU parameters W of Fig. 4. The ET process $(^4I_{13/2}, {}^3H_4) \rightarrow (^4I_{15/2}, {}^3F_3)$ is larger than the ET process $(^4I_{11/2}, {}^3H_4) \rightarrow (^4I_{15/2}, {}^1G_4)$, because the oscillator-strength product $(^4I_{15/2} \leftrightarrow {}^4I_{13/2}) \times (^3H_4 \leftrightarrow {}^3F_3)$ of 84000×10^{16} is significantly larger than the product $(^4I_{15/2} \leftrightarrow {}^4I_{11/2}) \times (^3H_4 \leftrightarrow {}^1G_4)$ of 924×10^{16}. The same result is found experimentally when comparing the ET parameters of Table I or Fig. 6(b). This explains the large difference in the lifetime quenching of the Er^{3+} $^4I_{13/2}$ and $^4I_{11/2}$ levels by the Pr^{3+} codopant [Fig. 6(a)].

For the calculation of the oscillator-strength product of the CR processes $(^2H_{11/2}, {}^4I_{15/2}) \rightarrow (^4I_{9/2}, {}^4I_{13/2})$ and $(^2H_{11/2}, {}^4I_{15/2}) \rightarrow (^4I_{13/2}, {}^4I_{9/2})$, the following considerations are made. First, the product is the sum of the oscillator-strength products of the two individual processes. Second, the Stark components of the $^2H_{11/2}$ level have a combined room-temperature Boltzmann population of typically 10% of the thermally coupled $^4S_{3/2}/{}^2H_{11/2}$ levels. Third, also CR from $^4S_{3/2}$ may occur. Since this process requires the absorption of one phonon, i.e., it is an energetically-endothermic process, its probability is typically an order-of-magnitude smaller[4] than for a process with a direct spectral overlap of its emission and absorption lines or an exothermic process which leads to the emission of one phonon. In this way, we find with the data of Table II that the overall CR process has a combined oscillator-strength product of 2133×10^{16}.

In Table III, the relative strengths of the five investigated ETU, CR, and ET parameters are compared to each other with respect to their experimental values (W parameters of Table I) and the above oscillator-strength products (obtained from the data of Table II). Experimentally as well as in the simplified model, transfer processes from the Er^{3+} $^4I_{13/2}$ level are the strongest processes whereas processes originating in the Er^{3+} $^4I_{11/2}$ level are relatively weak.

TABLE III. Relative strengths of the ETU, CR, and ET parameters (decreasing from top to bottom). Left-hand side: ordering of the W parameters of Table I; right-hand side: ordering of the oscillator-strength products obtained from the data of Table II.

No.	Measured	Calculated
1	ET from $^4I_{13/2}$	ET from $^4I_{13/2}$
2	ETU from $^4I_{13/2}$	ETU from $^4I_{13/2}$
3	CR from $^4S_{3/2}/{}^2H_{11/2}$	CR from $^4S_{3/2}/{}^2H_{11/2}$
4	ET from $^4I_{11/2}$	ETU from $^4I_{11/2}$
5	ETU from $^4I_{11/2}$	ET from $^4I_{11/2}$

We find, however, that there is not a total qualitative agreement between the experimental data and the simplified model concerning the ordering of the process strengths. The ETU and ET processes from $^4I_{11/2}$ do not have the same ordering in the experiment and the model. This may be due to the fact that the value of the $^4I_{11/2} \leftrightarrow {}^4F_{7/2}$ transition is different from the assumption made in Table II. Another possible reason might be that, in addition to the dependence on their oscillator-strength products, the transfer parameters also depend on the overlap integral of the corresponding absorption and emission lines.[2] However, the influence of the integral seems to be rather weak, because the possible assistance of phonons may smoothen the overlap.[4]

In general, the comparison in Table III shows that the product of the oscillator strengths of the emission and absorption transitions involved in an energy transfer process gives a reasonable indication of its strength which is expressed by its macroscopic transfer parameter W.

B. Comparison with $LiYF_4$:Er^{3+}

Recently, the same method as applied here was used to measure the parameters of ETU from the Er^{3+} $^4I_{13/2}$ and $^4I_{11/2}$ levels in $LiYF_4$ (Ref. 37) for different dopant concentrations of 5, 10, 15, 20, 30, and 32 at.%, and curves were fitted to derive equations for the concentration dependence of the ETU parameters. We compare here the values of these ETU parameters in $LiYF_4$ and ZBLAN for an Er^{3+} concentration of $8 \times 10^{20}\,cm^{-3}$ (= 5.8 at.% in $LiYF_4$ or 5 mol% in ZBLAN). Since the rate–equation sets used in the two publications are slightly different from each other, the data for the ETU parameters α of Ref. 37 have to be divided by two to compare to our W parameters.

In general, it is found that the values of the ETU parameters are of the same order-of-magnitude in $LiYF_4$ and ZBLAN. In particular, for ETU from $^4I_{13/2}$, the data of Ref. 37 provide a value of $W_{ETU} = 1.7 \times 10^{-17}\,cm^3/s$ in $LiYF_4$, which is approximately half of the value of $W_{ETU} = 2.8 \times 10^{-17}\,cm^3/s$ in ZBLAN (Table I). For ETU from $^4I_{11/2}$, the situation is reversed. In $LiYF_4$ a value of $W_{ETU} = 1.6 \times 10^{-17}\,cm^3/s$ is derived, whereas the value in ZBLAN, $W_{ETU} = 1.0 \times 10^{-17}\,cm^3/s$ (Table I), is almost a factor of 2 smaller.

For the operation of the Er^{3+} 3-μm laser (Fig. 1), the above comparison provides the following result: At the Er^{3+}

concentrations investigated here, the ratio of the probabilities of ETU from the $^4I_{13/2}$ lower laser level, which recycles energy to the $^4I_{11/2}$ upper laser level, vs. ETU from the $^4I_{11/2}$ upper laser level, which depletes inversion, is more favorable for ZBLAN compared to $LiYF_4$. The highest slope efficiency of the laser system is obtained at the Er^{3+} concentration at which the ratio of the probabilities of these ETU processes is largest.[20] This optimum Er^{3+} concentration is probably smaller in ZBLAN than the optimum concentration of $2\times10^{21}\,cm^{-3}(=15\,at.\%)$ in $LiYF_4$ (Refs. 18, 37).

C. Concentration dependence

The parameters of ETU and ET from the $^4I_{13/2}$ and $^4I_{11/2}$ levels as well as CR from the $^4S_{3/2}/^2H_{11/2}$ levels increase with increasing Er^{3+} concentration. The slopes in double-logarithmic representation are close to linear in all the five cases (Fig. 4). In contrast, the parameters of ET from the Er^{3+} $^4I_{13/2}$ and $^4I_{11/2}$ levels to the Pr^{3+} codopant are almost insensitive to Pr^{3+} concentration [Fig. 6(b)], i.e., the parameters of the ET processes depend linearly on donor concentration but are almost independent of acceptor concentration. If the same dependence on donor and acceptor concentrations that is found for the ET processes holds true for Er^{3+}–Er^{3+} transfer processes such as ETU and CR, then the experimentally-observed linear dependence of these processes on Er^{3+} concentration (Fig. 4) is indeed expected, because Er^{3+} acts simultaneously as donor and acceptor in these cases. Thus, all the investigated transfer processes exhibit the same dependence on donor and acceptor concentrations.

A comprehensive study on migration-accelerated ET in rare-earth-doped glasses was performed in Ref. 41. The major conclusion of this study was that ET in glasses, in contrast to ET in crystalline host materials, cannot be described by migration-accelerated quenching theories such as the diffusion model[42] or the jump model.[42] The most notable deviation of the experimental findings from theoretical predictions was the unusual increase of the transfer parameter with donor concentration which, in the case of glasses, typically follows a square-law dependence in the static-quenching regime which saturates to a linear dependence in the kinetic, i.e., the migration-accelerated regime.

If we want to compare our results (ion densities treated in units of cm^{-3}) to the results of Ref. 41 and references therein (ion densities treated in units of 1), then we have to translate our W parameters (given in units of cm^3s^{-1}) to the transfer parameters of Ref. 41 (given in units of s^{-1}). This is done by multiplying the W parameter of a specific transfer process with the concentration of acceptor ions in the sample under investigation. For the ETU and CR processes, the W parameters are multiplied by the Er^{3+} concentration. It follows that the dependence on Er^{3+} concentration translates from linear (as observed in our experiments; Fig. 4) to quadratic in the unit system of Ref. 41. For the ET processes, the W parameters are multiplied by the Pr^{3+} concentration. The dependence on Er^{3+} concentration remains linear whereas the dependence on Pr^{3+} concentration translates from independent to linear in the unit system of Ref. 41. Again, all the investigated transfer processes exhibit the same dependence on donor and acceptor concentrations, because we have only transformed the unit system.

When comparing the translated dependence of the transfer parameters on donor concentration with the results of Ref. 41, we find that the linear dependence corresponds to the migration-accelerated regime where the dependence of the transfer parameter on donor concentration saturates. In those glasses investigated in Ref. 41, this regime was observed for donor concentration above 10^{20}–$10^{21}\,cm^{-3}$, depending on glass composition. Our samples have donor concentrations of $2-14\times10^{20}\,cm^{-3}$. In the case of ET to Pr^{3+}, the acceptor concentrations of $0.4-2.5\times10^{20}\,cm^{-3}$ are also in the range typically used in Ref. 41, whereas in the case of ETU and CR within Er^{3+}, the acceptor concentrations are higher in our samples.

A possible reason for migration-accelerated transfer is the occurrence of active-ion clusters. Such clusters have been reported, e.g., for silica glasses.[43–45] Although the findings concerning the dependence of the transfer parameters on donor concentration in glasses are in agreement with the assumption that active-ion clusters occur in glass hosts,[41] the conclusion was drawn in Ref. 41 that clustering cannot be an explanation for the observed behavior. The reason for this conclusion was that similar results were found for all the glasses under investigation, despite the fact that these compositions were known to exhibit different degrees of segregation. For a comparison, fast energy migration between Er^{3+} ions was found to be present at dopant concentrations as small as $3.36\times10^{19}\,cm^{-3}(=1\,at.\%)$ in the crystalline material $Cs_3Lu_2Br_9$:Er^{3+} (Ref. 46), although there is currently no reason to assume that clustering of Er^{3+} ions occurs in this material.

The present data and the comparison with the results of other publications do not support the assumption that active-ion clusters are present in ZBLAN glass. The strong quenching of the Er^{3+} $^4I_{13/2}$ lifetime by the Pr^{3+} codopant can be explained by the large oscillator strength of the corresponding Pr^{3+} absorption transition. Also the comparison with transfer processes in $LiYF_4$:Er^{3+} does not reveal significantly-enhanced transfer parameters in ZBLAN:Er^{3+}. The comparison with migration-accelerated transfer in other glasses and a crystalline material shows that this phenomenon is typically observed at the dopant concentrations under investigation and is not necessarily related to the occurrence of active-ion clustering. However, the presence of active-ion clusters cannot be excluded by the investigations of this article.

V. CONCLUSIONS

In the ZBLAN glass host, we have measured the intrinsic lifetimes of the Er^{3+} $^4I_{13/2}$, $^4I_{11/2}$, and $^4S_{3/2}/^2H_{11/2}$ levels as well as the parameters of ETU from $^4I_{13/2}$ and $^4I_{11/2}$, ET from these levels to the Pr^{3+} $^3F_3$ and $^1G_4$ levels, respectively, and CR from the thermally-coupled Er^{3+} $^4S_{3/2}/^2H_{11/2}$ levels. The results show that ETU is as efficient in ZBLAN glass as in $LiYF_4$. Due to the higher oscillator strengths of the corresponding emission and absorption transitions, ETU and ET processes originating in the $^4I_{13/2}$ level have generally a higher probability than those from the $^4I_{11/2}$ levels.

The concentration dependence of the transfer parameters indicate that, at the dopant concentrations under investigation, transfer processes occur in the migration-accelerated regime. From the presented data, the presence of Er^{3+} ion clusters in ZBLAN cannot be excluded.

The lifetimes as well as the parameters of ETU, CR, and ET have been determined over a range of Er^{3+} and Pr^{3+} concentrations applicable to the design of double-clad diode-pumped Er^{3+} 3-μm fiber lasers operating on the $^4I_{11/2} \rightarrow {}^4I_{13/2}$ transition.[27–29,31] The consequences of our results for the operation of the Er^{3+} fiber laser are as follows. Codoping the system with Pr^{3+} is the preferred technique for a diode-pumped 3-μm fiber laser when high Er^{3+} concentrations for efficient ETU from the lower laser level are unavailable. Relatively small amounts of Pr^{3+} rapidly deplete the lower laser level while having a much lesser effect on the upper laser level. This allows the system to operate as a simple four-level laser with short lower and longer upper-state lifetimes.[47]

For Er^{3+} concentrations up to 8.75 mol% used in this investigation, ETU has approximately a factor of 3 larger probability for the lower laser level as compared to the upper laser level. These values are more favorable than those of $LiYF_4$:Er^{3+}, i.e., efficient ETU from the lower laser level can be achieved in ZBLAN without significantly quenching the upper laser level. With the future availability of highly Er^{3+}-doped fibers, ETU from the lower laser level can upconvert ions back to the upper laser level. This energy recycling regime with its inherent enhancement of the slope efficiency by a factor of two will, thus, be an attractive alternative to Pr^{3+} codoping at higher dopant concentrations.

ACKNOWLEDGMENTS

This work was financially supported by Engineering and Physical Sciences Research Council. M. Pollnau is indebted to Hans-Ulrich Güdel from the Department of Chemistry and Biochemistry, University of Bern, Switzerland, for his support.

*On leave from: Department of Chemistry and Biochemistry, University of Bern, Freiestrasse 3, CH-3012 Bern, Switzerland.

[1] T. Förster, Ann. Phys. (N.Y.) **2**, 55 (1948); Z. Naturforsch. B **49**, 321 (1949).
[2] D. L. Dexter, J. Chem. Phys. **21**, 836 (1953).
[3] M. Malinowski, B. Jacquier, M. Bouazaoui, M. F. Joubert, and C. Linares, Phys. Rev. B **41**, 31 (1990).
[4] S. R. Lüthi, M. Pollnau, H. U. Güdel, and M. P. Hehlen, Phys. Rev. B **60**, 162 (1999).
[5] M. Wermuth and H. U. Güdel, Chem. Phys. Lett. **281**, 81 (1997).
[6] M. Pollnau, P. J. Hardman, M. A. Kern, W. A. Clarkson, and D. C. Hanna, Phys. Rev. B **58**, 16076 (1998).
[7] G. Rustad and K. Stenersen, IEEE J. Quantum Electron. **32**, 1645 (1996).
[8] T. Y. Fan, G. Huber, R. L. Byer, and P. Mitzscherlich, IEEE J. Quantum Electron. **24**, 924 (1988).
[9] P. Laporta, S. De Silvestri, and V. Magni, Opt. Lett. **16**, 1952 (1991).
[10] D. S. Knowles and H. P. Jenssen, IEEE J. Quantum Electron. **28**, 1197 (1992).
[11] J. Schneider, D. Hauschild, C. Frerichs, and L. Wetenkamp, Int. J. Infrared Millim. Waves **15**, 1907 (1994).
[12] R. Paschotta, P. R. Barber, A. C. Tropper, and D. C. Hanna, J. Opt. Soc. Am. B **14**, 1213 (1997).
[13] P. E.-A. Möbert, A. Diening, E. Heumann, G. Huber, and B. H. T. Chai, Laser Phys. **8**, 214 (1998).
[14] L. Esterowitz and R. Allen, SPIE **1048**, 129 (1989).
[15] S. L. Jacques and G. Gofstein, SPIE **1427**, 63 (1991).
[16] M. Ith, H. Pratisto, H. J. Altermatt, M. Frenz, and H. P. Weber, Appl. Phys. B: Lasers Opt. **59**, 621 (1994).
[17] K. S. Bagdasarov, V. I. Zhekov, V. A. Lobachev, T. M. Murina, and A. M. Prokhorov, Kvant. Elektron. (Moscow) **10**, 452 (1983) [Sov. J. Quantum Electron. **13**, 262 (1983)].
[18] T. Jensen, A. Diening, G. Huber, and B. H. T. Chai, Opt. Lett. **21**, 585 (1996).
[19] D. W. Chen, C. L. Fincher, T. S. Rose, F. L. Vernon, and R. A. Fields, Opt. Lett. **24**, 385 (1999).
[20] M. Pollnau, R. Spring, Ch. Ghisler, S. Wittwer, W. Lüthy, and H. P. Weber, IEEE J. Quantum Electron. **32**, 657 (1996).
[21] Ch. Wyss, W. Lüthy, H. P. Weber, P. Rogin, and J. Hulliger, Opt. Commun. **139**, 215 (1997).
[22] M. Pollnau, Ch. Ghisler, W. Lüthy, and H. P. Weber, Appl. Phys. B: Lasers Opt. **67**, 23 (1998).
[23] R. S. Quimby, W. J. Miniscalco, and B. Thompson, SPIE **1581**, 72 (1991).
[24] S. Bedö, M. Pollnau, W. Lüthy, and H. P. Weber, Opt. Commun. **116**, 81 (1995).
[25] M. Pollnau, Ch. Ghisler, G. Bunea, M. Bunea, W. Lüthy, and H. P. Weber, Appl. Phys. Lett. **66**, 3564 (1995).
[26] M. Pollnau, Ch. Ghisler, W. Lüthy, H. P. Weber, J. Schneider, and U. B. Unrau, Opt. Lett. **22**, 612 (1997).
[27] M. Pollnau, IEEE J. Quantum Electron. **33**, 1982 (1997).
[28] B. Srinivasan, J. Tafoya, and R. K. Jain, Opt. Express **4**, 490 (1999).
[29] S. D. Jackson, T. A. King, and M. Pollnau, Opt. Lett. **24**, 1133 (1999).
[30] S. D. Jackson and T. A. King, Opt. Lett. **23**, 1462 (1998).
[31] T. Sandrock, D. Fischer, P. Glas, M. Leitner, M. Wrage, and A. Diening, Opt. Lett. **24**, 1284 (1999).
[32] T. Sandrock, A. Diening, and G. Huber, Opt. Lett. **24**, 382 (1999).
[33] W. R. Bosenberg, W. S. Pelouch, and C. L. Tang, Appl. Phys. Lett. **55**, 1952 (1989).
[34] L. Wetenkamp, G. F. West, and H. Többen, J. Non-Cryst. Solids **140**, 25 (1992).
[35] V. K. Bogdanov, W. E. K. Gibbs, D. J. Booth, J. S. Javorniczky, P. J. Newman, and D. R. MacFarlane, Opt. Commun. **132**, 73 (1996).
[36] M. D. Shinn, W. A. Sibley, M. G. Drexhage, and R. N. Brown, Phys. Rev. B **27**, 6635 (1983).
[37] T. Jensen, Ph.D. thesis, Institute of Laser-Physics, University of Hamburg, Germany, 1996.
[38] B. A. Wilson, J. Hegarty, and W. M. Yen, Phys. Rev. Lett. **41**, 268 (1978).
[39] L. Wetenkamp, Ph.D. thesis, Institute of High-Frequency Technique, Technical University of Braunschweig, Germany, 1991.
[40] C. Li, Y. Guyot, C. Linarès, R. Moncorgé, and M. F. Joubert, in *OSA Proceedings on Advanced Solid-State Lasers*, edited by A.

A. Pinto and T. Y. Fan (Optical Society of America, Washington, DC, 1993), Vol. 15, pp. 91–95.
[41] V. P. Gapontsev and N. S. Platonov, Mater. Sci. Forum **50**, 165 (1989).
[42] A. I. Burshtein, Usp. Fiz. Nauk **143**, 553 (1984) [Phys. Usp. **143**, 501 (1984)].
[43] R. S. Quimby, W. J. Miniscalco, and B. Thompson, J. Appl. Phys. **76**, 4472 (1994).
[44] E. Maurice, G. Monnom, B. Dussardier, and D. B. Ostrowsky, Opt. Lett. **20**, 2487 (1995).
[45] H. L. An, E. Y. B. Pun, H. D. Liu, and X. Z. Lin, Opt. Lett. **23**, 1197 (1998).
[46] M. P. Hehlen, G. Frei, and H. U. Güdel, Phys. Rev. B **50**, 16264 (1994).
[47] S. D. Jackson, T. A. King, and M. Pollnau, J. Mod. Opt. (unpublished).